EFDA–JET–CP(10)02/04

C. Brault, C. Gil, A. Boboc, P. Spuig and JET EFDA contributors

Numerical Processing of the Tore Supra Polarimetry Signals

Numerical Processing of the Tore Supra Polarimetry Signals

C. Brault[1], C. Gil[1], A. Boboc[2], P. Spuig[1] and JET EFDA contributors*

JET-EFDA, Culham Science Centre, OX14 3DB, Abingdon, UK

[1]Association EURATOM-CEA, IRFM, 13108 St Paul-lez-Durance, France
[2]EURATOM-CCFE Fusion Association, Culham Science Centre, OX14 3DB, Abingdon, OXON, UK
** See annex of F. Romanelli et al, "Overview of JET Results",*
(Proc. 22 nd IAEA Fusion Energy Conference, Geneva, Switzerland (2008)).

Preprint of Paper to be submitted for publication in Proceedings of the
International Conference on Plasma Diagnostics, Pont-à-Mousson, Frannce.
(12th April 2010 - 16th April 2010)

ABSTRACT.

On Tore Supra, a far infrared polarimeter diagnostic has been routinely used for diagnosing the current density by measuring the Faraday rotation angle.

As this angle is a few dozen of degrees on present plasma fusion devices, a high precision is needed to correctly reconstruct the current profile.

In this article, we present numerical methods to calculate the phase and the amplitude. A new method of phase shifting calculation is described. The validations have been made using the Tore Supra and JET polarimetry signals in comparing the calculated signals with the signals coming from analogue cards.

These methods have been developed to be used on the future numerical cards that will replace the Tore Supra present analogue ones.

1. INTRODUCTION

In magnetic fusion, the poloidal current control is a key factor to optimize the confinement and thus to reach the Lawson criteria. FIR polarimetric diagnostics have been developed to measure the current but still need to be improved to reach the required precisions and reliabilities [1]. On Tore Supra, and other plasma fusion devices [2], the polarimeter has an operating range of a few dozen of degrees for the Faraday rotation angles, with an accuracy of about 0.2^{o}. To be useful to a correct reconstruction of the current profiles, the accuracy needs to reach 0.06^{o}, which is compatible with the relative precision chosen for ITER (0.2^{o} accuracy but 40^{o} Faraday rotation angles [3]).

This article describes the numerical methods used to calculate the phase and the amplitude of the polarimetry signals. These methods have been validated by using Tore Supra and JET experimental signals.

2. PRINCIPLE OF THE POLARIMETRY

On Figure 1 is shown the method used on Tore Supra to determine the polarisation of the beam by a two detector technique [4,5]: the 195µm IR incoming linearly polarised beam crosses the plasma and is thus rotated by the Faraday Effect due to the electron density and the magnetic field: the polarisation direction of a linearly polarised wave crossing a magnetised plasma rotates by an angle:

$$\alpha_F = C.\lambda^2.\int n_e B_{//}.dz$$

Where λ is the wavelength, n_e the electron density, $B_{//}$ the magnetic field parallel to the beam propagation, C a constant and the integral is extended over the beam path [4]. By inversion of this integral relation, the poloidal magnetic field and consequently the current density profile can be deduced.

But the polarimetric angles are also affected by the Cotton-Mouton effect which makes elliptic the polarisation and is sensitive to the square of the magnetic field $B_\perp$ perpendicular to the propagation, inducing a phase difference:

$$\varphi_{cm} = C_2 \lambda^3 . \int n_e . \mathrm{B}^2 . dl$$

The beam is then recombined with a 100kHz shifted in frequency beam. A grid separates the two perpendicular polarisation components before they reach the two detectors. The detectors are semi-conductor InSb bolometers that are implanted in helium-cooled cryostats.

The two measured 100kHz signals are then multiplied by a synchronous amplifier to determine the rotation of the polarisation and the differential phase shift.

As the rotation is characterized by the change of amplitudes on the detectors, a calibration set is needed, which is constituted of a half wave quartz plate, to evaluate the response of the detectors to a known rotation.

But the main difficulty is to avoid spurious differential misalignments between the two detectors during plasmas.

They can be induced by the moves of mirrors or plasma refraction. This imposes to install the grid as near as possible at an equal distance from the cryostat geometry. The minimal distance from the grid to the detector is presently typically 50 centimetres on Tore Supra [6].

When a linearly polarised incident wave (the probing beam) crosses magnetized plasma, its state of polarisation changes by combination the Faraday and the Cotton-Mouton effects. This state of polarisation can be fully described by two equivalent couples of angles (Figure 2):

- ψ_P the **azimuth**, angle between the ellipse major axis and the *X* direction, and χ_P the **ellipticity**, angle given by the major and the minor axis (independent coordinate), and
- θ_P the **elevation**, angle given by the maxima of the two components on X and Y, and ϕ_P the **phase difference** between them.

At Tore Supra (as well as at other plasma fusion devices), the Faraday rotation angle (i.e. the Ψ_P angle, also called the α_F angle) is deduced from the amplitude ratios of the two detectors for the two orthogonal polarisation components of the 195µm probing beam wave.

As the Faraday rotation angle is at most ten degrees on Tore Supra, we obtain the relation:

$$tan\,(\Psi_p) = tan\,(\theta_p)\,cos\,(\phi_p) = \frac{B}{A}\,cos\,(\phi_p) = \frac{ABcos(\phi_p)}{A^2}$$

with *A* the amplitude of the first signal coming from the detectors and *B* the amplitude of the second one.

The Faraday angle is theoretically deduced from the measurement of $ABcos(\phi_P)$ and A^2. But a constant residual phase difference ϕ_0 exists in the diagnostic, due the optics and the electronic cards. The measured phase difference is no more ϕ_P but $(\phi_P - \phi_0)$, giving a new formula:

$$tan\,(\Psi_p) \approx \frac{ABcos(\phi_p - \phi_0)}{A^2} = \frac{ABcos(\phi_p)}{A^2}\ cos(\phi_0)...$$

$$... + \frac{ABsin(\phi_p)}{A^2}\ sin(\phi_0)...$$

This phase difference ϕ_0 is calculated during the diagnostic calibration, as well as calibration coefficients K_i (by 3rd degree polynomial fit [7]) to correct the losses due to the optics and the detector's response:

$$\alpha_F \approx (\sum_{i=1}^{3} K_i . \left[\frac{ABcos(\phi_p - \phi_0)}{A^2}\right]^i$$

3. THE ANALOGUE ELECTRONIC CARDS USED ON TORE SUPRA AND JET

A. TORE SUPRA

The 100kHz signals used on Tore Supra can be written $A.cos(\omega t)$ and $B.cos(\omega t+\phi_P)$, with w the frequency of the probing beam. The electronic cards have been designed to calculate the phase ϕ_P and the amplitudes A and B, which are obtained by using a DC to RMS conversion. $ABcos(\phi_P)$ and ABsin(ϕ_P) are calculated by synchronous multiplication and filtering to keep only the constant part.

To obtain $ABsin(\phi_P)$, the first input signal $B.cos(\omega t+\phi_P)$ is phase shifted of $\Pi/2$, in order to become $B.sin(\omega t+\phi_P)$. This operation is made by integration. Automatic correction is performed to take into account the integrator's response.

B. JET

The two 100kHz signals used on JET can be written [8]:

$$i(t) = E_X \cos(\omega t)$$
$$p(t) = E_Y \cos(\omega t - \phi)$$

where E_x and E_y are the amplitude, ω the frequency of the probing beam and ϕ the phase between the two signals. The analogue electronic cards evaluate the signals by multiplication and integration according to

$$\mathrm{PSD} = \ (p(t)\ \mathrm{x}\ i(t))\ (\propto \mathrm{E_x\,E_y}\ cos\ \phi)$$
$$\mathrm{PSP} = \ (p(t)\ \mathrm{x}\ i'(t))\ (\propto \mathrm{E_x\,E_y}\ sin\ \phi)$$
$$\mathrm{RMS} = \ (i(t)\ \mathrm{x}\ i(t))\ (\propto \mathrm{E_x^2})$$
$$\mathrm{RMS} = \ (i'(t)\ \mathrm{x}\ i'(t))\ (\propto \mathrm{E'^2_x})$$

where $i'(t)$ is obtained from $i(t)$ by a phase shift of 90°. From these signals, two ratios are used to calculate the phase and the faraday angle:

$$R = \frac{\mathrm{PSD}}{\mathrm{RMS}} \qquad R' = \frac{\mathrm{PSP}}{\sqrt{\mathrm{RMS.RMP}}}$$

4. NUMERICAL METHODS

On Figure 3 is shown the methods used to calculate the same signals as the analogue electronic card's ones. The first step is to digitalize the analogue signal. To have a good precision, we need to choose a sampling rate higher than the frequency of the studied signal. The beam frequency is around 100kHz, we have chosen a sampling frequency of 1MHz.

The A^2 or B^2 values are obtained by a direct multiplication of the digitalized signal by itself, and then by filtering the result. This filter is a smooth function, but a low-pass filter can be used as well.

The $ABcos(\phi_P)$ signal is calculated by the same method, by multiplying the two input signals.

The calculation of $ABsin(\phi_P)$ is more difficult. The first possible method is to interpolate the second input signal to shift the time of a quarter of its period. A cosines signal is thus transformed into a sinus signal.

This method by interpolation has defaults due to sampling frequency sensitivity. With a 1MHz sampling rate, the error on the amplitude of the signal can reach more than 4.5%, which is incompatible with the precision to be achieved. A second inconvenient is that the interpolation is not easy to program on a numerical processing card.

We have developed an other numerical method based on an N points' shift of the digitalized signal. This method is shown on Figure 4.

With these three points, we can calculate all the signals needed to evaluate the Faraday angle:

$$\mathrm{A}^2 = 2 \text{ x } (M_1.M_1)$$

$$ABcos\,(\Phi_p) = 2 \text{ x } (M_2.M_3)$$

$$ABcos\,(\Phi_p) = \frac{(M_1.M_3).\cos[\omega.(t_2 - t_1)] - (M_2.M_3)}{\sin[\omega.(t_2 - t_1)]}$$

where ω is the known frequency of the signal. The precision of this method is not sensitive to the sampling frequency and can be easily programmed in a numerical card.

5. APPLICATION TO EXPERIMENTAL SIGNALS

To validate these numerical methods, we have used experimental signals from Tore Supra and JET. The inputs and outputs of the analogue card have been recorded by using a numerical oscilloscope.

The sampling frequency is 1MHz.

A. TORE SUPRA

The signals have been recorded during the calibration and the plasma pulse, where the amplitude variations are very important (during the calibration, a half-wavelength plate rotates from -15^o to $+15^o$ to simulate the rotation of the polarisation of the probing beam,).

On Figure 5 are shown the results of the calculations. $ABsin(\phi_P)$ has been calculated with a 1 point shift (corresponding to a 37° phase shift). For both signals we observe a decrease of the noise for the calculated signal (red).

Moreover the mean values are different for the two signals (around 100mV). These differences will be taken into account for A or $ABcos\ (\phi_P)$ by the diagnostic calibration, but not for $ABsin(\phi_P)$, as $sin(\phi_P)$ is almost null during the calibration (Figure 6a).

The validation of the numerical calculation method is obtained from an other comparison: the conservation of the equality $(ABcos^2\ (\phi_P) + ABsin^2\ (\phi_P)/\ (A^2B^2) = 1$.

This equality must be verified during the calibration (Figure 6a: rotation of the plate: from −6° to +6°) and the plasma pulse. On Figure 6 one can see that for the experimental data, the equality is not verified. An important difference appears during the calibration (b), corresponding to a B value near zero. The numerical signal is better, its value is 1 except when B is near zero where its value is 0.97. During the plasma the experimental value is around 1.6. The numerical result is better with a value equals to 1.

B. JET

On Figure 7 are shown the results of the calculations using the JET input signals during the calibration (20−25s) and during plasma pulse (40−65s). Unlike the Tore Supra cards, the JET ones present a gain and sometimes an offset for each output. To compare the results of the calculations with the experimental data, we have determined the gain by fitting the calibration peak, and adjusted the offset using the time after the calibration and before the plasma (30−40s).

For PSD signal, one can see a good agreement between calculations and experimental data. The global behaviour is the same and only small differences appear during the plasma. These differences can be due to an initial phase ϕ_0 affecting the experimental data and differently calculated by the numerical method.

For the PSP signal, the gain has not been calculated during the calibration but during the plasma. One can see a good agreement between the blue and the red curve during this phase but not during the calibration. Nevertheless one can calculate that the error on the Faraday angle measurement, due to these small differences, is around 0.2^o.

On Figure 8 we can see the results for the conservation of $(ABcos^2(\phi_P)+ ABsin^2(\phi_P)/(A^2B^2)=1$. On JET, the B signal is not calculated, so we can't compare the numerical result with an experimental one. The equality is verified during the calibration (t < 25s) and is also verified during the plasma pulse (30s < t < 65s), except when B is near zero at t = 54s as the signals are very noisy at the end of this pulse.

CONCLUSION AND PERSPECTIVES

These results for Tore Supra and JET confirm that the numerical calculation can be used to calculate the Faraday angle with a higher precision than the Tore Supra analogue cards. The signal/noise ratio is better and the method is simple enough to be programmed on a numerical processing card.

A prototype card based on the FPGA technology is foreseen to validate this real-time numerical method of the Faraday angle measurement. It will be tested on Tore Supra and it could be of interest to test it on JET as well.

ACKNOWLEDGEMENTS

This work, supported by the European Communities under the contract of Association between EURATOM and CEA, was carried out within the framework of the European Fusion Development Agreement. The views and opinions expressed herein do not necessarily reflect those of the European Commission.

REFERENCES

[1]. T. Aniel and al: Proc EPS 2002

[2]. M. Brombin, A. Boboc, L. Zabeo, A. Murari: Real-time electron density measurements from Cotton–Mouton effect in JET machine, Review of Scientific Instruments **79**, (2008) 10E718

[3]. A. J. H. Donné, M. F. Graswinckel and al : Poloidal Polarimeter for current density measurements in ITER, Review of Scientific Instruments **75**, 11 (2004) 4694-4701

[4]. E. Joffrin, P. Desfrasne, C. Gil, D. Lapeyre: Polarimetry on Tore Supra, EUR-CEA-FC-1553 –1995

[5]. D. Elbeze, C. Gil, F. Imbeaux: Integration off the new reflected channels of the Tore Supra polarimeter for current analysis: 33th EPS conference, Roma 2006.

[6]. C. Gil, D. Elbeze and al: Retro-reflected Channels of the Tore Supra FIR Interfero-Polarimeter for the long Pulse Operation, Fusion Engineering and Design **56-57** (2001) 969-973

[7]. D. Elbeze, C. Gil, R. Giannella: Proc EPS 2001

[8]. K. Guenther and JET-EFDA contributors: Complete far-infrared polarimetry measurements at JET, 31st EPS conference, London 2004

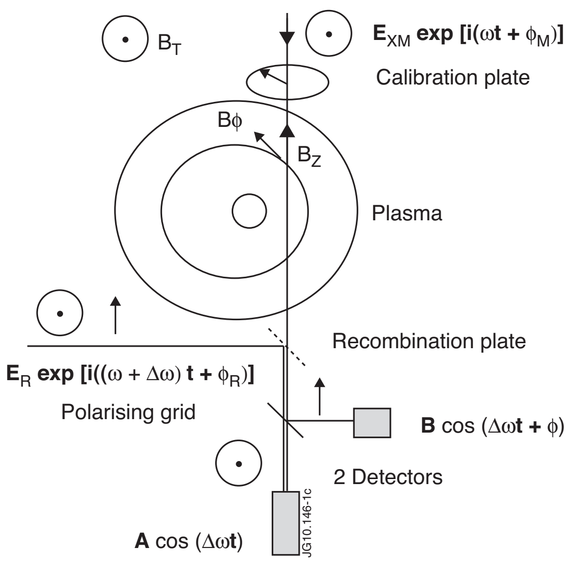

Figure 1: Synoptic of the Tore Supra Polarimeter.

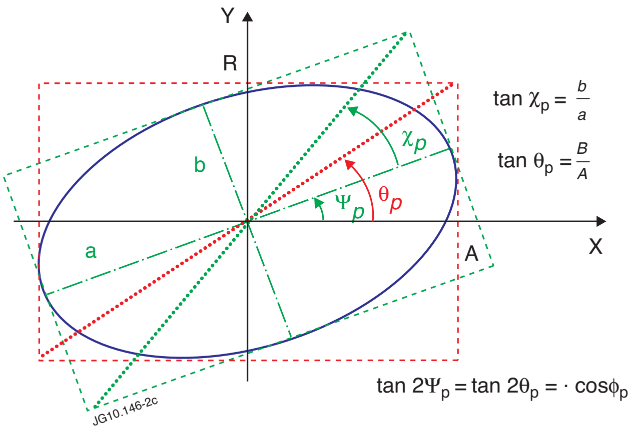

Figure 2: The polarisation ellipse of the probing beam.

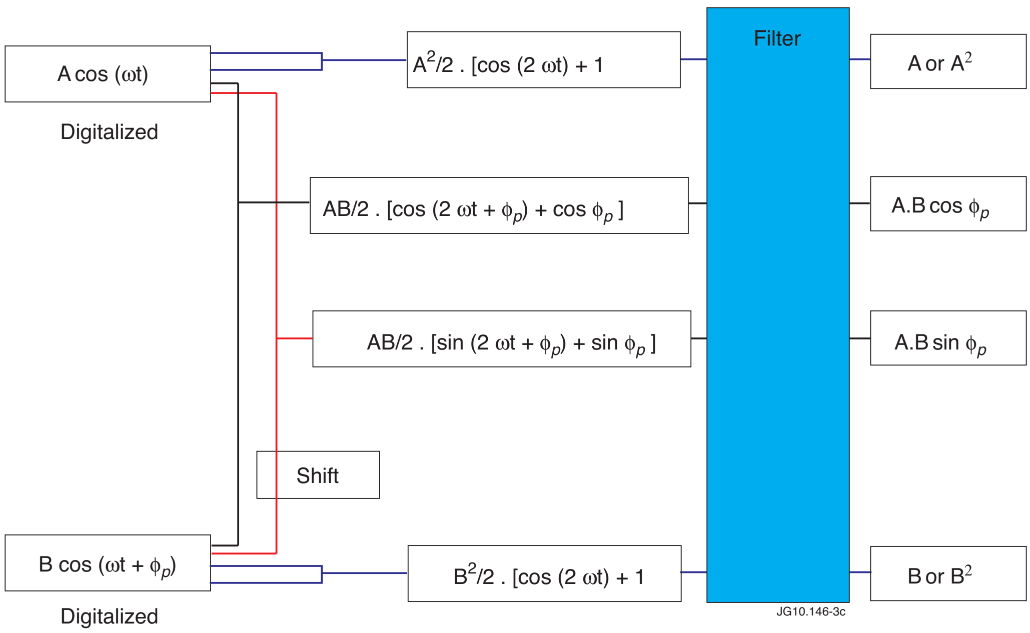

Figure 3: Numerical methods to calculate the Faraday angle.

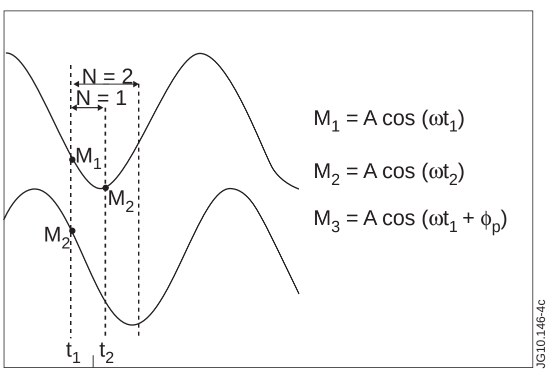

Figure 4: N points' shift calculation method

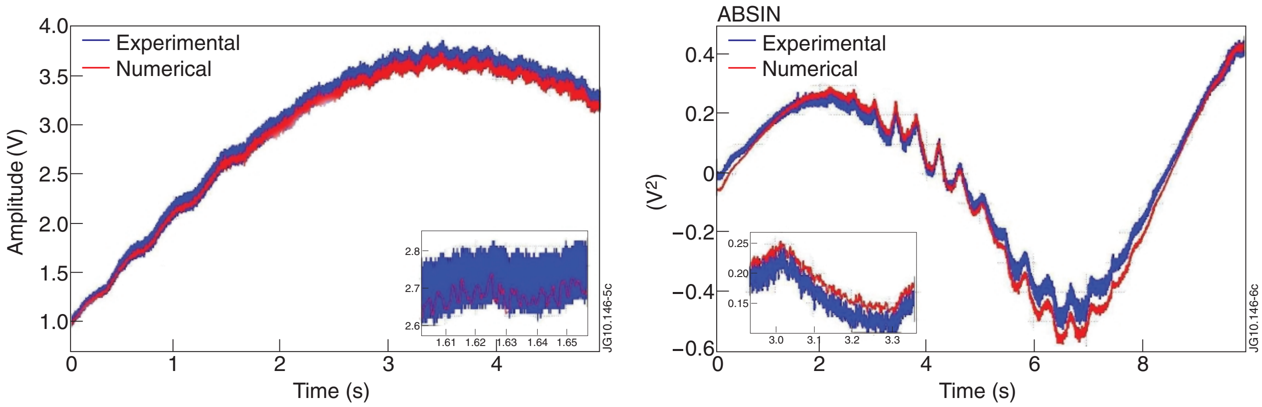

Figure 5: Comparison between Experimental data (blue) and calculation (red) for Tore Supra A and ABSIN signals

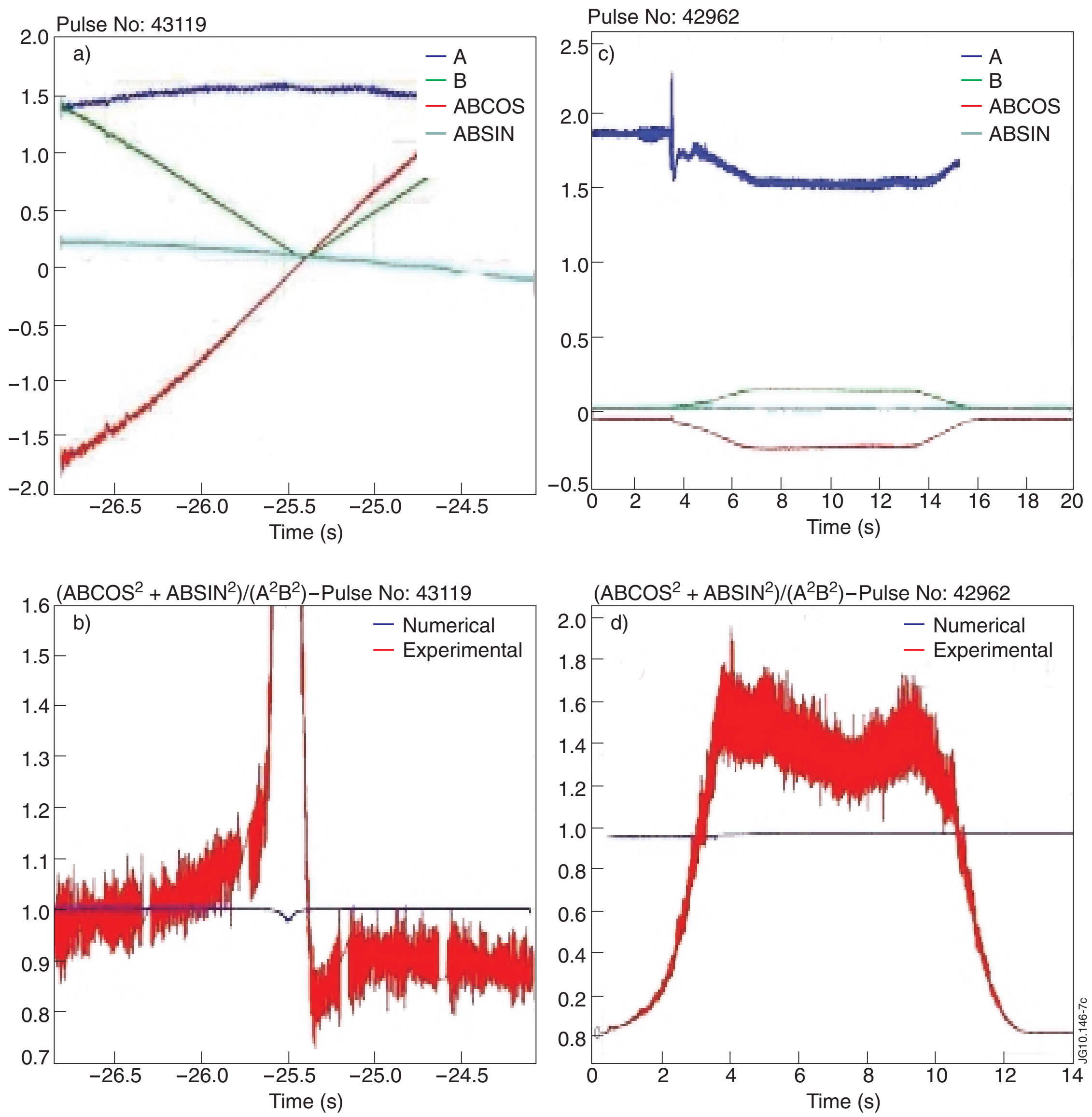

Figure 6: Conservation of $(ABCOS^2+ABSIN^2)/A^2B^2 = 1$ during a calibration (a,b) and a plasma pulse (c,d) on Tore Supra.

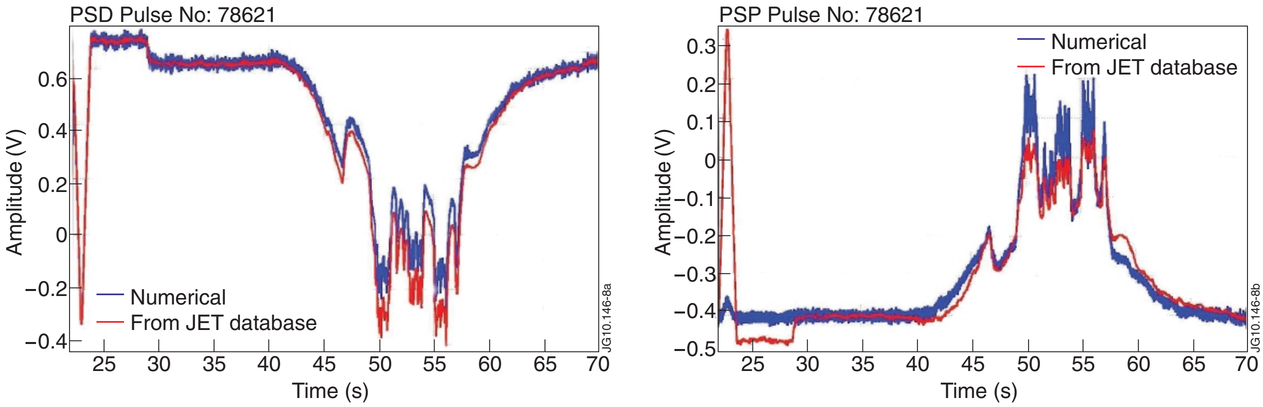

Figure 7: Comparison between Numerical (blue) and JET database signals (red) for PSD and PSP signals.

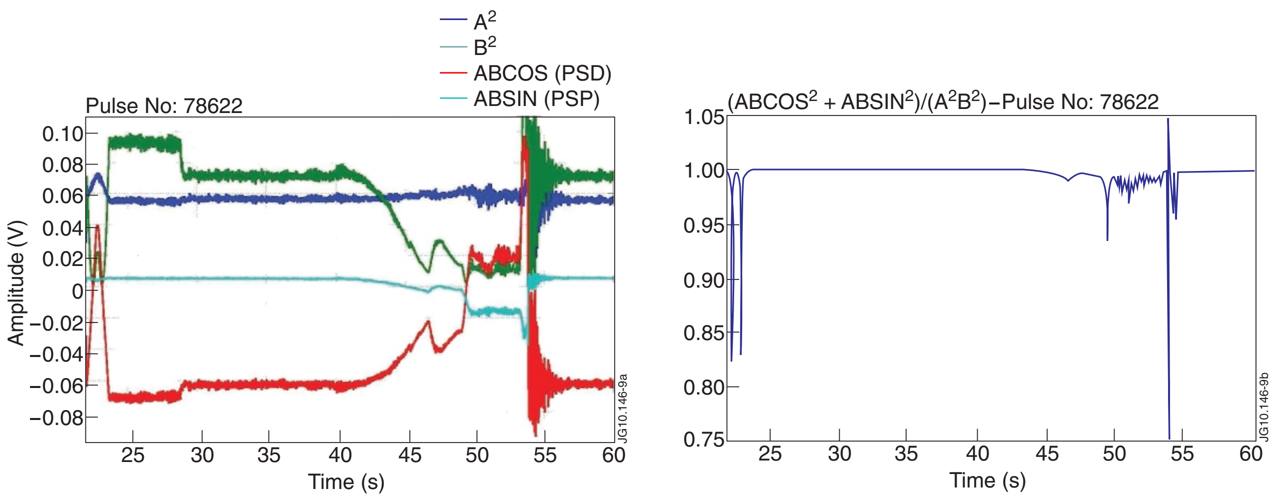

Figure 8: Conservation of $(ABCOS^2 + ABSIN^2)/A^2B^2 = 1$ on JET.